DMD Fast Forward. Published on April 11, 2023 as DOI: 10.1124/dmd.123.001310
This article has not been copyedited and formatted. The final version may differ from this version.

Variants of Flavin-containing Monooxygenase 3 (FMO3) Found in Subjects in an Updated Database of Genome Resources

Miaki Makiguchi, Makiko Shimizu, Yuka Yokota, Erika Shimamura, Eiji Hishinuma, Sakae Saito, Masahiro Hiratsuka, and Hiroshi Yamazaki*

Laboratory of Drug Metabolism and Pharmacokinetics, Showa Pharmaceutical University, Tokyo, Japan (M.M., M.S., Y.Y., E.S., H.Y.), Advanced Research Center for Innovations in Next-Generation Medicine and Tohoku Medical Megabank Organization, Tohoku University, Sendai, Japan (E.H., S.S., M.H.), and Graduate School of Pharmaceutical Sciences, Tohoku University and Department of Pharmaceutical Sciences, Tohoku University Hospital, Sendai, Japan (M.H.)

Running title: Polymorphisms of *FMO3* in Japanese cohorts

[*]**Corresponding Author**. Laboratory of Drug Metabolism and Pharmacokinetics, Showa Pharmaceutical University, 3-3165 Higashi-Tamagawa Gakuen, Machida, Tokyo 194-8543, Japan. Phone: +81-42-721-1406. Fax: +81-42-721-1406. E-mail address: hyamazak@ac.shoyaku.ac.jp

Abbreviations

FAD, flavin adenine dinucleotide

FMO3, flavin-containing monooxygenase 3.

Number of text pages: 26

Number of tables: 3

Number of figures: 3

Number of references: 30

Number of words in abstract: 250 words

Number of words in significance statement: 78 words

Number of words in introduction: 437 words

Number of words in discussion: 991 words

DMD Fast Forward. Published on April 11, 2023 as DOI: 10.1124/dmd.123.001310
This article has not been copyedited and formatted. The final version may differ from this version.

Abstract

Single-nucleotide substitutions of human flavin-containing monooxygenase 3 (*FMO3*) identified in the whole-genome sequences of the updated Japanese population reference panel (now containing 38,000 subjects) were investigated. In this study, 2 stop codon mutations, 2 frameshifts, and 43 amino-acid-substituted *FMO3* variants were identified. Among these 47 variants, 1 stop codon mutation, 1 frameshift, and 24 substituted variants were already recorded in the National Center for Biotechnology Information database. Functionally impaired FMO3 variants are known to be associated with the metabolic disorder trimethylaminuria; consequently, the enzymatic activities of the 43 substituted FMO3 variants were investigated. Twenty-seven recombinant FMO3 variants expressed in bacterial membranes had similar activities toward trimethylamine *N*-oxygenation (~75–125%) to that of wild-type FMO3 (98 min^{-1}). However, 6 recombinant FMO3 variants (Arg51Gly, Val283Ala, Asp286His, Val382Ala, Arg387His, and Phe451Leu) had moderately decreased (≈50%) activities toward trimethylamine *N*-oxygenation, and 10 recombinant FMO3 variants (Gly11Asp, Gly39Val, Met66Lys, Asn80Lys, Val151Glu, Gly193Arg, Arg387Cys, Thr453Pro, Leu457Trp, and Met497Arg) showed severely decreased FMO3 catalytic activity (<10%). Because of the known deleterious effects of FMO3 *C*-terminal stop codons, the four truncated FMO3 variants (Val187SerfsTer25, Arg238Ter, Lys416SerfsTer72, and Gln427Ter) were suspected to be inactive with respect to trimethylamine *N*-oxygenation. The FMO3 p.Gly11Asp and p.Gly193Arg variants were located within the conserved sequences of flavin adenine dinucleotide (positions 9–14) and NADPH (positions 191–196) binding sites, which are important for FMO3 catalytic function. Whole-genome sequence data and kinetic analyses revealed that 20 of the 47 nonsense or missense *FMO3* variants had moderately or

DMD Fast Forward. Published on April 11, 2023 as DOI: 10.1124/dmd.123.001310
This article has not been copyedited and formatted. The final version may differ from this version.

severely impaired activity toward *N*-oxygenation of trimethylaminuria.

DMD Fast Forward. Published on April 11, 2023 as DOI: 10.1124/dmd.123.001310
This article has not been copyedited and formatted. The final version may differ from this version.

Significance Statement

The number of single-nucleotide substitutions in human *FMO3* recorded in the expanded Japanese population reference panel database was updated. One novel stop mutation, *FMO3* p.Gln427Ter; one novel frameshift (p.Lys416SerfsTer72); and 19 novel amino-acid-substituted *FMO3* variants were identified, along with p.Arg238Ter, p.Val187SerfsTer25, and 24 amino-acid-substituted variants already recorded with individual rs numbers. Recombinant FMO3 Gly11Asp, Gly39Val, Met66Lys, Asn80Lys, Val151Glu, Gly193Arg, Arg387Cys, Thr453Pro, Leu457Trp, and Met497Arg variants showed severely decreased FMO3 catalytic activity, possibly associated with the metabolic disorder trimethylaminuria.

DMD Fast Forward. Published on April 11, 2023 as DOI: 10.1124/dmd.123.001310
This article has not been copyedited and formatted. The final version may differ from this version.

Introduction

Drug oxidation reactions in humans are mainly catalyzed by cytochrome P450 (P450, EC 1.14.14.1) and flavin-containing monooxygenase (FMO) enzymes (Rendic et al., 2022; Yamazaki and Shimizu, 2023). Genetic variations in these drug-metabolizing enzymes may result in altered pharmacokinetics and unexpected therapeutic responses (Guengerich, 2023). Genetic variations of P450 3A4 and drug interactions between P450 3A substrates/inhibitors may lead to an increased incidence of skeletal muscle or hepatic toxicity of the 3-hydroxy-3-methylglutaryl coenzyme A reductase inhibitor atorvastatin (Adachi et al., 2022). FMOs (EC 1.14.13.8) are a family of NADPH-dependent enzymes that oxygenate a wide range of heteroatom-containing substances (Krueger and Williams, 2005; Cashman and Zhang, 2006) including typical medicinal substrates (Nakamaru et al., 2014) and food-derived odorous trimethylamine (Shimizu et al., 2009). Phenotype–genotype analyses and the increasing availability of mega-databases have revealed the impaired human flavin-containing monooxygenase 3 (*FMO3*) variants associated with the metabolic disorder trimethylaminuria (Yamazaki et al., 2007; Shimizu et al., 2019b; Shimizu et al., 2021a; Shimizu et al., 2022).

In 2012, to foster reconstruction after the 2011 Great East Japan Earthquake, the Tohoku Medical Megabank Organization at Tohoku University established an advanced medical system in the form of a biobank that combines medical and genomic information. Because interindividual variability in P450 3A4 activity is a frequent cause of reduced drug efficacy and increased adverse effects, this biobank was previously searched for P450 3A4 variants. Wild-type P450 3A4 and 40 variants (including 11 new variants) were detected among the 4700 Japanese individuals contained in the biobank at the time of the study (Kumondai et al.,

DMD Fast Forward. Published on April 11, 2023 as DOI: 10.1124/dmd.123.001310
This article has not been copyedited and formatted. The final version may differ from this version.

2021). An increasing number of single-nucleotide substitutions in the human *FMO3* gene are being recorded in mega-databases (Shimizu et al., 2019b; Shimizu et al., 2021a; Shimizu et al., 2022). Furthermore, a series of reliable FMO3 genotyping confirmation methods has been assembled and developed for approximately 40 impaired FMO3 variants (Shimizu et al., 2021b). The Japanese population reference panel of the Tohoku Medical Megabank Organization's biobank was increased to 38,000 subjects (38K JPN) in 2022 from the previous panel that covered 8300 subjects (previous panels were known as 3.5K, 4.7K, and 8.3K JPN) (Shimizu et al., 2019b; Shimizu et al., 2021a; Shimizu et al., 2022). The current study aimed to identify impaired *FMO3* variants in this updated mega-database.

The current study followed our previous surveys of genetic FMO3 variants identified in extensive databases (Shimizu et al., 2019b; Shimizu et al., 2021a; Shimizu et al., 2022). Here, we report the detection of 20 important functionally impaired *FMO3* variants among the 47 *FMO3* mutations identified. Subjects harboring these variant *FMO3* genes may be susceptible to low drug clearances caused by impaired FMO3 function.

DMD Fast Forward. Published on April 11, 2023 as DOI: 10.1124/dmd.123.001310
This article has not been copyedited and formatted. The final version may differ from this version.

Materials and Methods

New *FMO3* Variant Information

Novel and previously reported *FMO3* single-nucleotide variants were identified (**Table 1)** in the whole-genome sequences present in the Japanese population reference panel (38K JPN) of the Tohoku Medical Megabank Organization (Sendai, Japan). The scope of the new panel has increased to 38,000 subjects from the previous panel that included 8300 subjects (Shimizu et al., 2019b; Shimizu et al., 2021a; Shimizu et al., 2022).

Recombinant FMO3 Proteins in Bacterial Membranes

Variant FMO3 cDNAs were prepared as previously described (Shimizu et al., 2019b; Shimizu et al., 2021a; Shimizu et al., 2023) using a QuikChange Lightning Site-Directed Mutagenesis Kit (Stratagene, La Jolla, CA, USA) with the designated 43 sets of primers (**Table 2)** and the FMO3 wild-type cDNA**.** Recombinant FMO3 proteins were expressed in *Escherichia coli* strain JM109 using the pTrc99A vector system (Pharmacia Biotechnology, Milwaukee, WI, USA) (Shimizu et al., 2019b; Shimizu et al., 2021a; Shimizu et al., 2023). The amounts of variant FMO3 proteins (0.1–200 pmol/mg protein) in the bacterial membrane fractions were determined immunochemically using an anti-FMO3 antibody (ab126790, Abcam, Cambridge, UK) and a human FMO3 standard (Corning, Woburn, MA, USA) (**Fig. 1)** as described previously (Shimizu et al., 2019b; Shimizu et al., 2021a; Shimizu et al., 2023).

Benzydamine and trimethylamine *N*-oxygenation rates by recombinant FMO3 proteins in the bacterial membranes (1.0 pmol equivalent FMO3) fortified with an NADPH-generating system and 1000 μM benzydamine (Sigma-Aldrich, St Louis, MO) and 25–1000 μM trimethylamine (Fujifilm Wako Pure Chemical, Osaka, Japan) in a final volume of 0.10 mL of 50 mM potassium phosphate buffer (pH 8.4) (Nagashima et al., 2009) at 37°C for 10 min in

DMD Fast Forward. Published on April 11, 2023 as DOI: 10.1124/dmd.123.001310
This article has not been copyedited and formatted. The final version may differ from this version.

triplicate were evaluated as described previously (Shimizu et al., 2015; Shimizu et al., 2019b; Shimizu et al., 2021a; Shimizu et al., 2023). Michaelis–Menten kinetic parameters for the *N*-oxygenation of trimethylamine by recombinant human FMO3 variant proteins (nmol product formation/min/nmol FMO3, i.e., min^{-1}) were calculated by nonlinear regression (mean ± standard error, n = 6 substrate concentrations, in triplicate determinations) using Prism 9 software (GraphPad Software, San Diego, CA, USA).

Variant Positions in Modeled FMO3 structure

A homology model for human FMO3 was previously constructed by Yeung et al. (Yeung et al., 2007) on the basis of the structure of yeast FMO using Molecular Operating Environment software (MOE 2022.02, Chemical Computing Group, Montreal, Canada) and was kindly provided to us by the authors. Key residues in the neighborhood of the NADPH and flavin adenine dinucleotide (FAD) cofactors of FMO3 were previously evaluated in that study. A schematic indicating the currently impaired FMO3 variants on the human FMO3 structure was rendered using MOE, and the common FMO3 Glu158Lys, Val257Met, and Glu308Gly variants were used as reference positions.

DMD Fast Forward. Published on April 11, 2023 as DOI: 10.1124/dmd.123.001310
This article has not been copyedited and formatted. The final version may differ from this version.

Results

New *FMO3* Variants

The Japanese population reference panel of the Tohoku Medical Megabank Organization was increased to 38,000 subjects in 2022 from the previous panel that included 8300 subjects (Shimizu et al., 2019b; Shimizu et al., 2021a; Shimizu et al., 2022). Among the forty-seven FMO3 variants found in the updated database in the current study, one novel stop codon mutation (p.Gln427Ter), one novel frameshift mutation (p.Lys416SerfsTer72), and 19 novel amino-acid-substituted *FMO3* variants were identified in the whole-genome sequence data in the updated 38K JPN database (**Table 1**). These were already tested variants *FMO3* p.Phe43Ile (Shimizu et al., 2015), p.Pro153GlnfsTer14 (Shimizu et al., 2019b), and p.Pro282Leu (Shimizu et al., 2019a) in addition. Among the novel 19 amino-acid-substituted *FMO3* variants, *FMO3* p.Met260Lys was recently reported in a compound variant found during phenotype–genotype analysis (Shimizu et al., 2023).

Additionally, p.Arg238Ter, p.Val187SerfsTer25, and 24 amino-acid substituted *FMO3* variants that were already recorded in the National Center for Biotechnology Information (NCBI) database with individual rs numbers were newly identified in the updated 38K JPN database (**Table 1**). Moreover, four functionally known amino-acid-substituted *FMO3* variants, namely *FMO3* p.Ser195Leu, p.Arg223Gln, and p.Ile441Thr [found in Japanese families (Shimizu et al., 2021b)] and *FMO3* p.Asn61Ser [reported in European families (Dolphin et al., 2000)] were also found in the updated 38K JPN database. Among the 24 already known amino-acid substituted *FMO3* variants, *FMO3* p.Ile37Thr (Teresa et al., 2006) and p.Arg387His (Kilic, 2017) have been reported in the literature, but their catalytic function remains unknown. Seventeen synonymous *FMO3* variants were also detected in this study:

DMD Fast Forward. Published on April 11, 2023 as DOI: 10.1124/dmd.123.001310
This article has not been copyedited and formatted. The final version may differ from this version.

c.51C>T, p.Ser17Ser; c.54C>A, p.Ile18Ile; c.120G>C, p.Leu40Leu; c.147G>A, p.Glu49Glu (rs 2101908646); c.207C>T, p.Phe69Phe; c.225C>T, p.Pro75Pro (rs 141235954); c.309C>T, p.Tyr103Tyr; c.450T>C, p.His150His (rs 1655715058); c.831C>A, p.Val277Val (rs 1656026830); c.834G>T, p.Leu278Leu (rs 2101921351); c.960G>A, p.Glu320Glu (rs 768813317); c.1134C>T, p.Ala378Ala; c.1152C>T, p.Leu384Leu (rs 1382743690); c.1332G>A, p.Lys444Lys (rs 962854254); c.1479G>A, p.Ser493Ser (rs 766383334); c.1539T>C, p.His513His (rs 771817026); and c.1587T>C, p.Leu529Leu. The allele frequency of all variants was <0.01%.

Recombinant FMO3 Variant Proteins

A total of 43 recombinant amino-acid-substituted FMO3 variants (**Table 1**), the functions of which have not yet been tested, and wild-type protein were recombinantly expressed in bacterial membranes (**Fig. 1**); the variant FMO3 cDNAs were prepared using the designated primers (**Table 2**). These variant FMO3 proteins (**Table 3**) were used to detect important *FMO3* variants that could result in low drug clearances because of impaired FMO3 function. The rates of benzydamine *N*-oxygenation at one substrate concentration mediated by recombinant FMO3 proteins were preliminary evaluated (**Table 3**). The rates of trimethylamine *N*-oxygenation mediated by recombinant FMO3 proteins in bacterial membranes (**Fig. 2**) were evaluated kinetically (**Table 3**). The results indicated that 27 recombinant variants had roughly similar activities (~75–125%) toward trimethylamine *N*-oxygenation to that of wild-type FMO3 (V_{max}, 98 min^{-1}; **Fig. 2A**), i.e., FMO3 Ile37Thr and Val110Ala (**Fig. 2B**), Pro70Ser and Glu136Gln (**Fig. 2C**), Met82Leu and Gln209Arg (**Fig. 2D**), Ile104Val and Val236Ile (**Fig. 2E**), Val145Phe and Thr241Asn (**Fig. 2F**), Asp253Glu and Asp253Val (**Fig. 2G**), Asn285Ser and Met260Lys (**Fig. 2H**), Met405Thr and Phe264Leu (**Fig.**

DMD Fast Forward. Published on April 11, 2023 as DOI: 10.1124/dmd.123.001310
This article has not been copyedited and formatted. The final version may differ from this version.

2I), Arg417Cys and Ile296Val (**Fig. 2J**), Arg417His and Leu361Ile (**Fig. 2K**), Leu399Ser (**Fig. 2L**), Met402Val (**Fig. 2M**), Ile447Val and Gly421Asp (**Fig. 2N**), Ser493Trp and Val474Leu (**Fig, 2O**), and Met497Val (**Fig. 2P**).

In contrast, six recombinant FMO3 variants had moderately decreased activities toward trimethylamine *N*-oxygenation, with approximately half the V_{max} value of wild-type FMO3: these were FMO3 Arg51Gly (**Fig. 2A**), Val283Ala (**Fig. 2H**), Asp286His (**Fig. 2I**), Val382Ala (**Fig. 2K**), Arg387His (**Fig. 2L**), Phe451Leu (**Fig. 2M**). Moreover, ten recombinant FMO3 variants, namely FMO3 Gly11Asp (**Fig. 2A**), Gly39Val (**Fig. 2B**), Met66Lys (**Fig. 2C**), Asn80Lys (**Fig. 2D**), Val151Glu (**Fig. 2E**), Gly193Arg (**Fig. 2F**), Arg387Cys (**Fig. 2L**), Thr453Pro (**Fig. 2N**), Leu457Trp (**Fig, 2O**), and Met497Arg (**Fig. 2P**), showed severely decreased FMO3 catalytic activities (< 10% of wild-type FMO3).

Location of Amino Acid Changes in Modeled Variant FMO3 Structure

The positions of substituted amino acids in the impaired FMO3 variants are illustrated as yellow/orange additions to the schematic of the molecular structure reported previously (**Fig. 3**). The homology model for human FMO3 that was previously constructed (Yeung et al., 2007), based on the structure of yeast FMO, was used to illustrate the locations of amino acid changes of the 20 moderately or seriously impaired FMO3 variants identified in the updated mega-database in this study. Newly identified impaired FMO3 variant amino acid substitutions were widely spread and were independent of the positions of FAD/NADPH cofactors in human FMO3.

DMD Fast Forward. Published on April 11, 2023 as DOI: 10.1124/dmd.123.001310
This article has not been copyedited and formatted. The final version may differ from this version.

Discussion

Trimethylamine is a selective substrate for human FMO3 (Lang et al., 1998). Wild-type FMO3 extensively catalyzes trimethylamine *N*-oxygenation to produce non-odorous (Shephard et al., 2012) but putatively proatherogenic (Hartiala et al., 2014) trimethylamine *N*-oxide. Because many *FMO3* variants associated with the metabolic disorder trimethylaminuria have been identified (Yamazaki and Shimizu, 2013), genetic testing based on traditional urinary phenotyping assays is a useful approach for the detection of homozygous/heterozygous carriers of deleterious *FMO3* variants (Shimizu et al., 2023). In this study, all 43 amino-acid-substituted *FMO3* variant cDNAs (**Table 2**) found in the updated population reference panel (**Table 1**) were expressed in bacterial membranes, and the presence of the resulting recombinant proteins were confirmed immunochemically (**Fig. 1**). The *FMO3* p.Met260Lys variant found in this study is also present in a novel compound *FMO3* variant p.(Glu158Lys; Met260Lys; Glu308Gly; Ile426Thr) that was separately identified in a 7-year-old girl (inherited from her mother) in a phenotype–genotype assay (Shimizu et al., 2023). Recombinant p.Met260Lys (**Fig. 2H**) and compound FMO3 p.(Glu158Lys; Met260Lys; Glu308Gly; Ile426Thr) variant proteins (Shimizu et al., 2023) showed mild and moderate decreases, respectively, in their capacity for trimethylamine *N*-oxygenation compared with wild-type FMO3. It should be noted that both single-variant information in the mega-database and compound variants forming new *FMO3* haplotypes in the family study findings should be a good battery system for understanding the increasing numbers of important human *FMO3* variants.

FMO3 is characterized by a stable 4a-flavin hydroperoxide intermediate capable of oxygenating nucleophiles and electrophiles even in the absence of a substrate (Jones and

DMD Fast Forward. Published on April 11, 2023 as DOI: 10.1124/dmd.123.001310
This article has not been copyedited and formatted. The final version may differ from this version.

Ballou, 1986), resulting in a theoretically similar Michaelis constant (K_m) for NADPH-dependent substrate oxygenation. As illustrated in **Fig. 3**, FMO3 contains a conserved primary sequence structure characteristic of the FAD binding site in the *N*-terminus region (GXGXXG motif at positions 9–14) and another conserved structure characteristic of the NADPH–pyrophosphate-binding site (GXGXXG motif at positions 191–196) (Krueger and Williams, 2005). In the present study, the *FMO3* p.Gly11Asp variant was detected in the updated 38K JPN genome panel (**Table 1**). Recombinant FMO3 p.Gly11Asp variant protein had a much lower activity toward trimethylamine than the wild-type FMO3 protein (<1% of the wild-type, **Fig. 2A**). The *FMO3* p.Gly193Arg variant within FMO3 positions 191–196 was also detected in the updated 38K JPN genome panel, in addition to the *FMO3* p.Gly191Asp previously found in the 8.3K JPN genome panel (Shimizu et al., 2022) and *FMO3* p.Gly191Cys (at the same 191 position) found in the 3.5K JPN database (Shimizu et al., 2019b). Furthermore, the *FMO3* p.Gly193Glu variant at the same position was detected in a patient (Chalmers et al., 2006), and the FMO3 p.Ser195Leu variant, which had decreased activity (<10% of wild-type FMO3), was identified in a previous phenotyping study (Shimizu et al., 2012). Because their substitution resulted in severely decreased FMO3 activity, Gly11, Gly191, Gly193, and Ser195, which occur inside the FAD- or NADPH-binding sites (Krueger and Williams, 2005), are evidently important amino acid residues for FMO3 catalytic function. The impaired *N*-oxidation activities toward trimethylamine by some FMO3 variants could be expanded to other drug substrates such as benzydamine (**Table 3**).

Met66 reportedly lies at an interface between the FAD binding domain and the *C*-terminal domain (Yeung et al., 2007), which is possibly optimal for adequate binding of FAD. At this Met66 position, the newly discovered *FMO3* p.Met66Lys variant (**Fig. 2C**) and previously

DMD Fast Forward. Published on April 11, 2023 as DOI: 10.1124/dmd.123.001310
This article has not been copyedited and formatted. The final version may differ from this version.

reported *FMO3* p.Met66Val and p.Met66Ile variants (resulting in low activities) were identified, respectively, in the 38K JPN databank (**Table 1**), in a Japanese family (Shimizu et al., 2021a) and in a British family (Akerman et al., 1999). Substitutions at the FMO3 Gly39 and Val151 residues analyzed in this study had low activities (**Fig. 2B** and **Fig. 2E**) and were also in close proximity to FAD in the current FMO3 homology model (**Fig. 3**). Recombinant FMO3 Arg387Cys (**Fig. 2L**) showed severely decreased FMO3 catalytic activity, whereas FMO3 Arg387His at the same position did not. Similar differential effects of substituted Cys and His on FMO3-mediated activity were also previously confirmed at Arg205, i.e., for Arg205Cys and Arg205His (Shimizu et al., 2019b).

The wild-type human FMO3 enzyme has 532 amino acids (**Fig. 3**), but some genetic polymorphisms in FMO3 encode naturally truncated forms that have little or no detectable functional enzymatic activity (Yamazaki et al., 2007; Shimizu et al., 2021b) because they are insufficient anchors to membranes that boost FMO3 function. The deleterious effects of the *C*-terminal stop codons (from Glu305 and Arg500 positions) on recombinant truncated FMO3 variant-mediated drug *N*-oxygenation (Yamazaki et al., 2007; Enna, 2012) suggest that truncated FMO3 variants Val187SerfsTer25, Arg238Ter, Lys416SerfsTer72, and Gln427Ter found in this study are also likely to be inactive for trimethylamine *N*-oxygenation.

The presence of novel *FMO3* variants, such as p.Gly191Cys, p.Met260Val, and p.Met260Lys, which were found both in mega-databanks and in phenotyping assays, can be easily confirmed by polymerase chain reaction–restriction fragment length polymorphism or allele-specific polymerase chain reaction methods using DNA fractions obtained from subject swabs, as described previously (Shimizu et al., 2021b; Shimizu et al., 2023). For example, the known p.Met260Val (c.778A>G, rs1201544644) *FMO3* variant and the new

DMD Fast Forward. Published on April 11, 2023 as DOI: 10.1124/dmd.123.001310
This article has not been copyedited and formatted. The final version may differ from this version.

p.Met260Lys (c.779T>A) *FMO3* variant can be detected separately and simply by using *Bfu*AI to give 378 / 240 + 138 (mutant) fragments and by using *Mbo*II to give 378 / 264 + 114 (mutant) fragments, respectively (Shimizu et al., 2023). This series of systems should facilitate the easy detection in the clinical setting of FMO3 variants in subjects susceptible to low drug clearance or drug interactions possibly caused by impaired FMO3 function. It would be useful if similar simple detection tools for newly identified impaired *FMO3* variants could be developed in the future. In conclusion, whole-genome sequence analysis data revealed 20 nonsense or missense *FMO3* variants (of the 47 *FMO3* mutations identified here) that were newly identified as having moderately or severely impaired activities toward the *N*-oxygenation of trimethylaminuria. Individuals with these *FMO3* variants identified in a Japanese cohort may be susceptible to modified drug clearances and drug interactions.

DMD Fast Forward. Published on April 11, 2023 as DOI: 10.1124/dmd.123.001310
This article has not been copyedited and formatted. The final version may differ from this version.

Acknowledgments

We thank Allan E. Rettie, Mizuki Harano, Moegi Matsuta, Yuria Nakamura, Saki Yoshioka, Haruka Nishimura, Koichiro Adachi, and Norie Murayama for their assistance. We are also grateful to David Smallbones for copyediting a draft of this article.

Data Availability Statement

The authors declare that all the data supporting the findings of this study are contained within the paper.

DMD Fast Forward. Published on April 11, 2023 as DOI: 10.1124/dmd.123.001310
This article has not been copyedited and formatted. The final version may differ from this version.

Authorship Contributions

Participated in research design: Yamazaki.

Conducted experiments: Makiguchi, Shimizu, Yokota, Shimamura.

Contributed new reagents or analytic tools: Hishinuma, Saito, Hiratsuka.

Performed data analysis: Makiguchi, Shimizu, Yamazaki.

Wrote or contributed to the writing of the manuscript: Makiguchi, Shimizu, Yamazaki.

DMD Fast Forward. Published on April 11, 2023 as DOI: 10.1124/dmd.123.001310
This article has not been copyedited and formatted. The final version may differ from this version.

References

Adachi K, Ohyama K, Tanaka Y, Sato T, Murayama N, Shimizu M, Saito Y, and Yamazaki H (2022) High hepatic and plasma exposures of atorvastatin in subjects harboring impaired cytochrome P450 3A4 *16 modeled after virtual administrations and possibly associated with statin intolerance found in the Japanese adverse drug event report database. *Drug Metab Pharmacokinet* **48:**100486.

Akerman BR, Forrest S, Chow L, Youil R, Knight M, and Treacy EP (1999) Two novel mutations of the FMO3 gene in a proband with trimethylaminuria. *Hum Mutat* **13:**376-379.

Cashman JR and Zhang J (2006) Human flavin-containing monooxygenases. *Annu Rev Pharmacol Toxicol* **46:**65-100.

Chalmers RA, Bain MD, Michelakakis H, Zschocke J, and Iles RA (2006) Diagnosis and management of trimethylaminuria (FMO3 deficiency) in children. *J Inherit Metab Dis* **29:**162-172.

Dolphin CT, Janmohamed A, Smith RL, Shephard EA, and Phillips IR (2000) Compound heterozygosity for missense mutations in the flavin-containing monooxygenase 3 (FMO3) gene in patients with fish-odour syndrome. *Pharmacogenetics* **10:**799-807.

Enna SJ (2012) Note to readers. *Biochem Pharmacol* **84:**411.

Guengerich FP (2023) Drug Metabolism: A Half-Century Plus of Progress, Continued Needs, and New Opportunities. *Drug Metab Dispos* **51:**99-104.

Hartiala J, Bennett BJ, Tang WH, Wang Z, Stewart AF, Roberts R, McPherson R, Lusis AJ, Hazen SL, Allayee H, and Consortium CA (2014) Comparative genome-wide association studies in mice and humans for trimethylamine N-oxide, a proatherogenic metabolite of choline and L-carnitine. *Arterioscler Thromb Vasc Biol* **34:**1307-1313.

Jones KC and Ballou DP (1986) Reactions of the 4a-hydroperoxide of liver microsomal flavin-containing monooxygenase with nucleophilic and electrophilic substrates. *J Biol Chem* **261:**2553-2559.

Kilic M (2017) Primary trimethylaminuria (fish odor syndrome) and hypothyroidism in an adolescent. *Turk J Pediatr* **59:**614-616.

Krueger SK and Williams DE (2005) Mammalian flavin-containing monooxygenases: structure/function, genetic polymorphisms and role in drug metabolism. *Pharmacol Ther* **106:**357-387.

Kumondai M, Gutierrez Rico EM, Hishinuma E, Ueda A, Saito S, Saigusa D, Tadaka S, Kinoshita K, Nakayoshi T, Oda A, Abe A, Maekawa M, Mano N, Hirasawa N, and Hiratsuka M (2021) Functional Characterization of 40 CYP3A4 Variants by Assessing Midazolam 1'-Hydroxylation and Testosterone 6beta-Hydroxylation. *Drug Metab Dispos* **49:**212-220.

Lang DH, Yeung CK, Peter RM, Ibarra C, Gasser R, Itagaki K, Philpot RM, and Rettie AE (1998) Isoform specificity of trimethylamine N-oxygenation by human flavin-containing monooxygenase (FMO) and P450 enzymes: selective catalysis by FMO3. *Biochem Pharmacol* **56:**1005-1012.

Nagashima S, Shimizu M, Yano H, Murayama N, Kumai T, Kobayashi S, Guengerich FP, and Yamazaki H (2009) Inter-individual variation in flavin-containing monooxygenase 3 in livers from Japanese: correlation with hepatic transcription factors. *Drug Metab Pharmacokinet* **24:**218-225.

Nakamaru Y, Hayashi Y, Ikegawa R, Kinoshita S, Perez Madera B, Gunput D, Kawaguchi A, Davies M, Mair S, Yamazaki H, Kume T, and Suzuki M (2014) Metabolism and disposition of the dipeptidyl peptidase IV inhibitor teneligliptin in humans. *Xenobiotica* **44:**242-253.

Rendic SP, Crouch RD, and Guengerich FP (2022) Roles of selected non-P450 human oxidoreductase enzymes in protective and toxic effects of chemicals: review and compilation of reactions. *Arch Toxicol* **96:**2145-2246.

Shephard EA, Treacy EP, and Phillips IR (2012) Clinical utility gene card for: trimethylaminuria. *Eur J Hum Genet* **20:**e1-e5.

Shimizu M, Hirose N, Kato M, Sango H, Uenuma Y, Makiguchi M, Hishinuma E, Saito S, Hiratsuka M, and Yamazaki H (2022) Further survey of genetic variants of flavin-containing monooxygenase 3 (FMO3) in Japanese subjects found in an updated database of genome resources and identified by phenotyping for trimethylaminuria. *Drug Metab Pharmacokinet* **46:**100465.

Shimizu M, Kobayashi Y, Hayashi S, Aoki Y, and Yamazaki H (2012) Variants in the flavin-containing monooxygenase 3 (FMO3) gene responsible for trimethylaminuria in a Japanese population. *Mol Genet Metab* **107:**330-334.

Shimizu M, Koibuchi N, Mizugaki A, Hishinuma E, Saito S, Hiratsuka M, and Yamazaki H (2021a) Genetic variants of flavin-containing monooxygenase 3 (FMO3) in Japanese subjects identified by phenotyping for trimethylaminuria and found in a database of genome resources. *Drug Metab Pharmacokinet* **38:**100387.

Shimizu M, Kozono M, Murayama N, and Yamazaki H (2009) Bonitos with low content of malodorous trimethylamine as palliative care for self-reported Japanese trimethylaminuria subjects. *Drug Metab Pharmacokinet* **24:**549-552.

Shimizu M, Mizugaki A, Koibuchi N, Sango H, Uenuma Y, and Yamazaki H (2021b) A series of simple detection systems for genetic variants of flavin-containing monooxygenase 3 (FMO3) with impaired function in Japanese subjects. *Drug Metab Pharmacokinet* **41:**100420.

Shimizu M, Origuchi Y, Ikuma M, Mitsuhashi N, and Yamazaki H (2015) Analysis of six novel flavin-containing monooxygenase 3 (FMO3) gene variants found in a Japanese population suffering from trimethylaminuria. *Mol Genet Metab Rep* **5:**89-93.

Shimizu M, Yamamoto A, Makiguchi M, Shimamura E, Yokota Y, Harano M, and Yamazaki H (2023) A family study of compound variants of flavin-containing monooxygenase 3 (FMO3) in Japanese subjects found by urinary phenotyping for trimethylaminuria. *Drug Metab Pharmacokinet* **48:**100490.

Shimizu M, Yoda H, Igarashi N, Makino M, Tokuyama E, and Yamazaki H (2019a) Novel variants and haplotypes of human flavin-containing monooxygenase 3 gene associated with Japanese subjects suffering from trimethylaminuria. *Xenobiotica* **49:**1244-1250.

Shimizu M, Yoda H, Nakakuki K, Saso A, Saito I, Hishinuma E, Saito S, Hiratsuka M, and Yamazaki H (2019b) Genetic variants of flavin-containing monooxygenase 3 (FMO3) derived from Japanese subjects with the trimethylaminuria phenotype and whole-genome sequence data from a large Japanese database. *Drug Metab Pharmacokinet* **34:**334-339.

Teresa E, Lonardo F, Fiumara A, Lombardi C, Russo P, Zuppi C, Scarano G, Musumeci S, and Gianfrancesco F (2006) A spectrum of molecular variation in a cohort of Italian families with trimethylaminuria: identification of three novel mutations of the FMO3 gene. *Mol Genet Metab* **88:**192-195.

Yamazaki H, Fujita H, Gunji T, Zhang J, Kamataki T, Cashman JR, and Shimizu M (2007) Stop codon mutations in the flavin-containing monooxygenase 3 (FMO3) gene responsible for trimethylaminuria in a Japanese population. *Mol Genet Metab* **90:**58-63.

Yamazaki H and Shimizu M (2013) Survey of variants of human flavin-containing monooxygenase 3 (FMO3) and their drug oxidation activities. *Biochem Pharmacol* **85:**1588-1593.

Yamazaki H and Shimizu M (2023) Species Specificity and Selection of Models for Drug

Oxidations Mediated by Polymorphic Human Enzymes. *Drug Metab Dispos* **51:**123-129.

Yeung CK, Adman ET, and Rettie AE (2007) Functional characterization of genetic variants of human FMO3 associated with trimethylaminuria. *Arch Biochem Biophys* **464:**251-259.

DMD Fast Forward. Published on April 11, 2023 as DOI: 10.1124/dmd.123.001310
This article has not been copyedited and formatted. The final version may differ from this version.

Footnotes

Funding

This work was supported partly by the Japan Society for the Promotion of Science Grant-in-Aid for Scientific Research 19K07205 and partly by Research Support Project for Life Science and Drug Discovery [Basis for Supporting Innovative Drug Discovery and Life Science Research (BINDS)] from the Japan Agency for Medical Research and Development (AMED) under grant no. JP22ama121019. Masahiro Hiratsuka was supported by a grant from AMED (grant no. JP19kk0305009).

Declarations of Interest

The authors have no competing interests to declare.

DMD Fast Forward. Published on April 11, 2023 as DOI: 10.1124/dmd.123.001310
This article has not been copyedited and formatted. The final version may differ from this version.

Figure legends

Fig. 1. **Immunoblot analysis of human FMO3 variant proteins expressed in *E. coli* membranes.** Immunoblotting was performed using commercially available anti-human FMO3 antibody. Abbreviated names and the number of micrograms of membrane protein per well of recombinant human FMO3 wild-type and variant proteins are indicated in the representative gels. Std is a recombinant human FMO3 protein standard that is commercially available.

Fig. 2. **Kinetic analysis of trimethylamine *N*-oxygenation mediated by recombinant FMO3 variant proteins.** Michaelis–Menten kinetic parameters for recombinant FMO3 proteins were calculated by curve fitting using nonlinear regression (mean ± standard error, n = 6 substrate concentrations, in triplicate determinations). (A) Data for FMO3 wild-type (circles) and variants FMO3 Arg51Gly (triangles) and FMO3 Gly11Asp (squares). (B) Data for variants FMO3 Ile37Thr (circles), FMO3 Val110Ala (triangles), and FMO3 Gly39Val (squares). (C) Data for variants FMO3 Pro70Ser (circles), FMO3 Glu136Gln (triangles), and FMO3 Met66Lys (squares). (D) Data for variants FMO3 Met82Leu (circles), FMO3 Gln209Arg (triangles), and FMO3 Asn80Lys (squares). (E) Data for variants FMO3 Ile104Val (circles), FMO3 Val236Ile (triangles), and FMO3 Val151Glu (squares). (F) Data for variants FMO3 Val145Phe (circles), FMO3 Thr241Asn (triangles), and FMO3 Gly193Arg (squares). (G) Data for variants FMO3 Asp253Glu (circles) and FMO3 Asp253Val (triangles). (H) Data for variants FMO3 Asn285Ser (circles), FMO3 Met260Lys (triangles), and FMO3 Val283Ala (squares). (I) Data for variants FMO3 Met405Thr (circles), FMO3 Phe264Leu (triangles), and FMO3 Asp286His (squares). (J) Data for variants FMO3 Arg417Cys (circles) and FMO3 Ile296Val (triangles). (K) Data for the FMO3 Arg417His (circles), FMO3

DMD Fast Forward. Published on April 11, 2023 as DOI: 10.1124/dmd.123.001310
This article has not been copyedited and formatted. The final version may differ from this version.

Leu361Ile (triangles), and FMO3 Val382Ala (squares). (L) Data for variants FMO3 Leu399Ser (circles), FMO3 Arg387His (triangles), and FMO3 Arg387Cys (squares). (M) Data for variants FMO3 Met402Val (circles) and FMO3 Phe451Leu (triangles). (N) Data for variants FMO3 Ile447Val (circles), FMO3 Gly421Asp (triangles), and FMO3 Thr453Pro (squares). (O) Data for variants FMO3 Ser493Trp (circles), FMO3 Val474Leu (triangles), and FMO3 Leu457Trp (squares). (P) Data for variants FMO3 Met497Val (circles) and FMO3 Met497Arg (squares).

Fig. 3. FMO3 variant positions illustrated in modeled molecular structure. The homology model for human FMO3 previously constructed based on the yeast FMO structure (Yeung et al., 2007) was used in this study. To illustrate the variety of locations of the 20 impaired FMO3 variants found in the updated 38K JPN mega-database in this study, their residue positions [yellow, including loss-of-function FMO3 variants (<10%) highlighted in orange], were superposed on those of the previously identified 43 FMO3 variant residue positions (white, including loss-of-function FMO3 variants highlighted in light grey). FAD/NADPH cofactors (dark grey) on human FMO3 were rendered, in addition to the three common FMO3 variants Glu158Lys, Val257Met, and Glu308Gly (green) as reference amino acid positions.

DMD Fast Forward. Published on April 11, 2023 as DOI: 10.1124/dmd.123.001310
This article has not been copyedited and formatted. The final version may differ from this version.

Table 1. Forty-seven *FMO3* variants found in the 38K JPN database updated from the previous panel that covered 8300 subjects.

Position	Change	Exon	dbSNP rs number	Amino acid change
				Wild type
171092690	c.32G>A	2		Gly11Asp
171092768	c.110T>C	2	rs1176032822	Ile37Thr
171092774	c.116G>T	2		Gly39Val
171103803	c.151A>G	3	rs765137570	Arg51Gly
171103849	c.197T>A	3		Met66Lys
171103860	c.208C>T	3		Pro70Ser
171103892	c.240C>A	3	rs759312959	Asn80Lys
171103896	c.244A>C	3	rs2101908859	Met82Leu
171103962	c.310A>G	3		Ile104Val
171107682	c.329T>C	4	rs376881697	Val110Ala
171107759	c.406G>C	4	rs780703747	Glu136Gln
171107786	c.433G>T	4		Val145Phe
171107805	c.452T>A	4		Val151Glu
171108152	c.559delG	5	rs1270775688	Val187SerfsTer25
171108171	c.577G>A	5	rs1655736434	Gly193Arg
171108220	c.626A>G	5	rs1571219503	Gln209Arg
171110876	c.706G>A	6	rs201271626	Val236Ile
171110882	c.712C>T	6	rs893223321	Arg238Ter
171110892	c.722C>A	6	rs1655878176	Thr241Asn
171110928	c.758A>T	6		Asp253Val
171110929	c.759C>A	6	rs1655881057	Asp253Glu
171110949	c.779T>A	6		Met260Lys*
171110960	c.790T>C	6		Phe264Leu
171114027	c.848T>C	7		Val283Ala
171114033	c.854A>G	7		Asn285Ser
171114035	c.856G>C	7	rs777342108	Asp286His
171114065	c.886A>G	7		Ile296Val
171114260	c.1081C>A	7		Leu361Ile
171114324	c.1145T>C	7	rs201860024	Val382Ala
171114338	c.1159C>T	7	rs145526965	Arg387Cys
171114339	c.1160G>A	7	rs72549331	Arg387His
171116220	c.1196T>C	8	rs2101924146	Leu399Ser
171116228	c.1204A>G	8	rs141117096	Met402Val
171116238	c.1214T>C	8		Met405Thr
171116266	c.1247delA	8		Lys416SerfsTer72

DMD Fast Forward. Published on April 11, 2023 as DOI: 10.1124/dmd.123.001310
This article has not been copyedited and formatted. The final version may differ from this version.

171116273	c.1249C>T	8	rs149551557	Arg417Cys
171116274	c.1250G>A	8	rs200985584	Arg417His
171117105	c.1262G>A	9	rs61757397	Gly421Asp
171117122	c.1279C>T	9		Gln427Ter
171117182	c.1339A>G	9	rs1656195641	Ile447Val
171117194	c.1351T>C	9		Phe451Leu
171117200	c.1357A>C	9	rs2101925375	Thr453Pro
171117213	c.1370T>G	9		Leu457Trp
171117263	c.1420G>C	9	rs1656201510	Val474Leu
171117321	c.1478C>G	9	rs61008738	Ser493Trp
171117332	c.1489A>G	9		Met497Val
171117333	c.1490T>G	9		Met497Arg

The allele frequency of all variants was <0.01%. The scope of the new panel has increased to 38,000 subjects from the previous panel that included 8300 subjects (Shimizu et al., 2019b; Shimizu et al., 2021a; Shimizu et al., 2022). Seventeen synonymous *FMO3* variants, c.51C>T, p.Ser17Ser; c.54C>A, p.Ile18Ile; c.120G>C, p.Leu40Leu; c.147G>A, p.Glu49Glu (rs 2101908646); c.207C>T, p.Phe69Phe; c.225C>T, p.Pro75Pro (rs 141235954); c.309C>T, p.Tyr103Tyr; c.450T>C, p.His150His (rs 1655715058); c.831C>A, p.Val277Val (rs 1656026830); c.834G>T, p.Leu278Leu (rs 2101921351); c.960G>A, p.Glu320Glu (rs 768813317); c.1134C>T, p.Ala378Ala; c.1152C>T, p.Leu384Leu (rs 1382743690); c.1332G>A, p.Lys444Lys (rs 962854254); c.1479G>A, p.Ser493Ser (rs 766383334); c.1539T>C, p.His513His (rs 771817026); and c.1587T>C, p.Leu529Leu were also detected. The complete human *FMO3* gene sequence given in GenBank [Genome Reference Consortium Human Build 38 (GRCh38) p13 chr 1, Accession Number NC_000001.11] was used as the reference. * Met260Lys was reported previously (Shimizu et al., 2023).

DMD Fast Forward. Published on April 11, 2023 as DOI: 10.1124/dmd.123.001310
This article has not been copyedited and formatted. The final version may differ from this version.

Table 2. Sequences of sets of primers used for mutagenesis of *FMO3*.

Primer	Sequence
Gly11Asp -S	5′- CCATCATTGGAGCTGATGTGAGTGGCTTGGC -3′
Gly11Asp -AS	5′- GCCAAGCCACTCACATCAGCTCCAATGATGG -3′
Ile37Thr -S	5′- GAAGAGCAATGACACTGGGGGCCTGTGG -3′
Ile37Thr -AS	5′- CCACAGGCCCCCAGTGTCATTGCTCTTC -3′
Gly39Val -S	5′- GCAATGACATTGGGGTCCTGTGGAAATTTTCAG -3′
Gly39Val -AS	5′- CTGAAAATTTCCACAGGACCCCAATGTCATTGC -3′
Arg51Gly -S	5′- CCATGCAGAGGAGGGCGGGGCTAGCATTTACAA -3′
Arg51Gly -AS	5′- TTTGTAAATGCTAGCCCCGCCCTCCTCTGCATGG -3′
Met66Lys -S	5′- CAACTCTTCCAAAGAGAAGATGTGTTTCCCAGAC -3′
Met66Lys -AS	5′- GTCTGGGAAACACATCTTCTCTTTGGAAGAGTTG -3′
Pro70Ser -S	5′- AAGAGATGATGTGTTTCTCAGACTTCCCATTTCCC -3′
Pro70Ser -AS	5′- GGGAAATGGGAAGTCTGAGAAACACATCATCTCTT -3′
Asn80Lys -S	5′- CCCGATGACTTCCCCAAATTTATGCACAACAGCAA -3′
Asn80Lys -AS	5′- TTGCTGTTGTGCATAAATTTGGGGAAGTCATCGGG -3′
Met82Leu -S	5′- CTTCCCCAACTTTCTGCACAACAGCAAG -3′
Met82Leu -AS	5′- CTTGCTGTTGTGCAGAAAGTTGGGGAAG -3′
Ile104Val -S	5′- GAACCTCCTGAAGTACGTACAATTTAAGACATTTG -3′
Ile104Val -AS	5′- CAAATGTCTTAAATTGTACGTACTTCAGGAGGTTC -3′
Val110Ala -S	5′- CAATTTAAGACATTTGCATCCAGTGTAAATAAAC -3′
Val110Ala -AS	5′- GTTTATTTACACTGGATGCAAATGTCTTAAATT -3′
Glu136Gln -S	5′- GGGATGGTAAAAAACAATCGGCTGTCTTTG -3′
Glu136Gln -AS	5′- CAAAGACAGCCGATTGTTTTTTACCATCCC -3′
Val145Phe -S	5′- GTCTTTGATGCTGTAATGTTTTGTTCCGGACATCA -3′
Val145Phe -AS	5′- TGATGTCCGGAACAAAACATTACAGCATCAAAGAC -3′
Val151Glu -S	5′- GTTCCGGACATCATGAGTATCCCAACCTACC -3′
Val151Glu -AS	5′- GGTAGGTTGGGATACTCATGATGTCCGGAAC -3′
Gly193Arg -S	5′- GGTTGGCCTGAGGAATTCGGG -3′
Gly193Arg -AS	5′- CCCGAATTCCTCAGGCCAACC -3′
Gln209Arg -S	5′- GCACAGCAGAACGGGTCATGATCAG -3′
Gln209Arg -AS	5′- CTGATCATGACCCGTTCTGCTGTGC -3′
Val236Ile -S	5′- CTTGGGACATGCTGCTCATCACTCGATTTGGAACC -3′
Val236Ile -AS	5′- GGTTCCAAATCGAGTGATGAGCAGCATGTCCCAAG -3′
Thr241Asn -S	5′- CACTCGATTTGGAAACTTCCTCAAGAAC -3′
Thr241Asn -AS	5′- GTTCTTGAGGAAGTTTCCAAATCGAGTG -3′
Asp253Val -S	5′- CGACAGCCATCTCTGTCTGGTTGTACGTGAA -3′
Asp253Val -AS	5′- TTCACGTACAACCAGACAGAGATGGCTGTCG -3′
Asp253Glu -S	5′- CGACAGCCATCTCTGAATGGTTGTACGTGAAGC -3′
Asp253Glu -AS	5′- GCTTCACGTACAACCATTCAGAGATGGCTGTCG -3′

Met260Lys -S*	5′- GTTGTACGTGAAGCAGAAGAATGCAAGATTCAAGC-3′
Met260Lys -AS*	5′- GCTTGAATCTTGCATTCTTCTGCTTCACGTACAAC-3′
Phe264Leu -S	5′- GCAGATGAATGCAAGACTCAAGCATGAAAACTA -3′
Phe264Leu -AS	5′- TAGTTTTCATGCTTGAGTCTTGCATTCATCTGC -3′
Val283Ala -S	5′- CCTGAGGAAAGAGCCTGCATTTAACGATGAGCTCC -3′
Val283Ala -AS	5′- GGAGCTCATCGTTAAATGCAGGCTCTTTCCTCAGG -3′
Asn285Ser -S	5′- AGCCTGTATTTAGCGATGAGCTCCC -3′
Asn285Ser -AS	5′- GGGAGCTCATCGCTAAATACAGGCT -3′
Asp286His -S	5′- AAGAGCCTGTATTTAACCATGAGCTCCCAGCAAGC -3′
Asp286His -AS	5′- GCTTGCTGGGAGCTCATGGTTAAATACAGGCTCTT -3′
Ile296Val -S	5′- CAAGCATTCTGTGTGGCGTTGTGTCCGTAAAGCCT -3′
Ile296Val -AS	5′- AGGCTTTACGGACACAACGCCACACAGAATGCTTG -3′
Leu361Ile -S	5′- GAGTATTTCCTCCTCTAATTGAGAAGTCAACCATA -3′
Leu361Ile -AS	5′- TATGGTTGACTTCTCAATTAGAGGAGGAAATACTC -3′
Val382Ala -S	5′- GCTGCCATTCCCACAGCTGACCTCCAGTCCCGC -3′
Val382Ala -AS	5′- GCGGGACTGGAGGTCAGCTGTGGGAATGGCAGC -3′
Arg387Cys -S	5′- CAGTTGACCTCCAGTCCTGCTGGGCAGCACAAGTA -3′
Arg387Cys -AS	5′- TACTTGTGCTGCCCAGCAGGACTGGAGGTCAACTG -3′
Arg387His -S	5′- GTTGACCTCCAGTCCCACTGGGCAGCACAAGTA -3′
Arg387His -AS	5′- TACTTGTGCTGCCCAGTGGGACTGGAGGTCAAC -3′
Leu399Ser -S	5′- GGGAACTTGTACTTCGCCTTCTATGGAAG -3′
Leu399Ser -AS	5′- CTTCCATAGAAGGCGAAGTACAAGTTCCC -3′
Met402Val -S	5′- CTTGTACTTTGCCTTCTGTGGAAGACATGATGAAT -3′
Met402Val -AS	5′- ATTCATCATGTCTTCCACAGAAGGCAAAGTACAAG -3′
Met405Thr -S	5′- GCCTTCTATGGAAGACACGATGAATGATATTAATG -3′
Met405Thr -AS	5′- CATTAATATCATTCATCGTGTCTTCCATAGAAGGC -3′
Arg417Cys -S	5′- GAAAATGGAGAAAAAGTGCAAATGGTTTGGCA -3′
Arg417Cys -AS	5′- TGCCAAACCATTTGCACTTTTTCTCCATTTTC -3′
Arg417His -S	5′- GAAAATGGAGAAAAAGCACAAATGGTTTGGCAA -3′
Arg417His -AS	5′- TTGCCAAACCATTTGTGCTTTTTCTCCATTTTC -3′
Gly421Asp -S	5′- GCGCAAATGGTTTGACAAAAGCGAGACC -3′
Gly421Asp -AS	5′- GGTCTCGCTTTTGTCAAACCATTTGCGC -3′
Ile447Val -S	5′- CAAAGCCCAACGTCCCATGGCTGT -3′
Ile447Val -AS	5′- ACAGCCATGGGACGTTGGGCTTTG -3′
Phe451Leu -S	5′- CATCCCATGGCTGCTTCTCACAGATC -3′
Phe451Leu -AS	5′- GATCTGTGAGAAGCAGCCATGGGATG -3′
Thr453Pro -S	5′- CCATGGCTGTTTCTCCCAGATCCCAAATTGG -3′
Thr453Pro -AS	5′- CCAATTTGGGATCTGGGAGAAACAGCCATGG -3′
Leu457Trp -S	5′- CTCACAGATCCCAAATGGGCCATGGAAGTTTAT -3′
Leu457Trp -AS	5′- ATAAACTTCCATGGCCCATTTGGGATCTGTGAG -3′
Val474Leu -S	5′- CTACCAGTTTAGGCTGCTGGGCCCAGGGCAGTG -3′

DMD Fast Forward. Published on April 11, 2023 as DOI: 10.1124/dmd.123.001310
This article has not been copyedited and formatted. The final version may differ from this version.

Val474Leu -AS	5′- CACTGCCCTGGGCCCAGCAGCCTAAACTGGTAG -3′
Ser493Trp -S	5′- ACCCAGTGGGACCGGTGGTTGAAACCCATGCAG -3′
Ser493Trp -AS	5′- CTGCATGGGTTTCAACCACCGGTCCCACTGGGT -3′
Met497Val -S	5′- CGGTCGTTGAAACCCGTGCAGACACGAGTGG -3′
Met497Val -AS	5′- CCACTCGTGTCTGCACGGGTTTCAACGACCG -3′
Met497Arg -S	5′- GGTCGTTGAAACCCAGGCAGACACGAGTGGT -3′
Met497Arg -AS	5′- ACCACTCGTGTCTGCCTGGGTTTCAACGACC -3′

* This primer set was reported previously (Shimizu et al., 2023).

DMD Fast Forward. Published on April 11, 2023 as DOI: 10.1124/dmd.123.001310
This article has not been copyedited and formatted. The final version may differ from this version.

Table 3. **Drug oxygenation activities mediated by recombinant FMO3 variant proteins.**

FMO3 protein	Expression level, pmol FMO3/mg protein	Benzydamine *N*-oxygenation, nmol/min/nmol FMO3 (at 1000 μM)	Trimethylamine *N*-oxygenation	
			K_m, μM	V_{max}, min^{-1}
Wild type	80	205	24 ± 2	98 ± 2
Gly11Asp	9	1.5	Not available	0.5 ± 0.1
Ile37Thr	70	210	19 ± 2	92 ± 2
Gly39Val	30	0.3	32 ± 22	0.5 ± 0.1
Arg51Gly	200	51	23 ± 3	36 ± 1
Met66Lys	7	2.5	89 ± 40	0.4 ± 0.1
Pro70Ser	110	212	36 ± 3	107 ± 2
Asn80Lys	0.1	1.7	38 ± 34	3.5 ± 0.6
Met82Leu	100	191	23 ± 2	118 ± 2
Ile104Val	70	192	23 ± 3	91 ± 3
Val110Ala	50	174	18 ± 2	75 ± 1
Glu136Gln	120	186	21 ± 2	78 ± 1
Val145Phe	90	204	22 ± 3	100 ± 3
Val151Glu	25	19	55 ± 7	13 ± 1
Gly193Arg	70	1.8	77 ± 42	1.7 ± 0.3
Gln209Arg	170	171	22 ± 3	79 ± 2
Val236Ile	160	144	18 ± 2	72 ± 1
Thr241Asn	170	169	28 ± 2	71 ± 1
Asp253Val	70	224	49 ± 7	89 ± 3
Asp253Glu	220	192	35 ± 2	101 ± 1
Met260Lys	200	138	32 ± 2	84 ± 1
Phe264Leu	170	186	24 ± 2	87 ± 1
Val283Ala	110	86	21 ± 2	44 ± 1
Asn285Ser	100	200	20 ± 3	98 ± 2
Asp286His	70	68	94 ± 9	41 ± 1

DMD Fast Forward. Published on April 11, 2023 as DOI: 10.1124/dmd.123.001310
This article has not been copyedited and formatted. The final version may differ from this version.

Ile296Val	200	180	26 ± 1	78 ± 1
Leu361Ile	200	195	34 ± 1	96 ± 1
Val382Ala	200	127	21 ± 2	67 ± 1
Arg387Cys	5	27	29 ± 4	11 ± 1
Arg387His	6	207	27 ± 3	49 ± 1
Leu399Ser	90	125	33 ± 3	79 ± 1
Met402Val	120	189	19 ± 2	80 ± 1
Met405Thr	100	158	36 ± 3	112 ± 2
Arg417Cys	110	196	33 ± 3	115 ± 2
Arg417His	130	186	24 ± 4	122 ± 5
Gly421Asp	190	148	44 ± 2	83 ± 1
Ile447Val	130	185	27 ± 3	91 ± 2
Phe451Leu	90	114	25 ± 3	62 ± 1
Thr453Pro	5	3.4	Not available	1.2 ± 0.2
Leu457Trp	3	2.1	36 ± 20	1.1 ± 0.1
Val474Leu	60	180	25 ± 3	74 ± 2
Ser493Trp	30	181	26 ± 4	95 ± 3
Met497Val	70	187	30 ± 3	92 ± 2
Met497Arg	20	7.1	17 ± 8	6.0 ± 0.4

Benzydamine *N*-oxygenation activities were determined at a substrate concentration of 1000 μM in triplicate. Michaelis–Menten kinetic parameters for recombinant FMO3 proteins were calculated by curve fitting using nonlinear regression (mean ± standard error, n = 6 substrate concentrations, in triplicate determinations). The K_m values for trimethylamine *N*-oxygenations not available were resulted from larger standard deviations than apparent K_m values calculated, because of low individual catalytic activities.

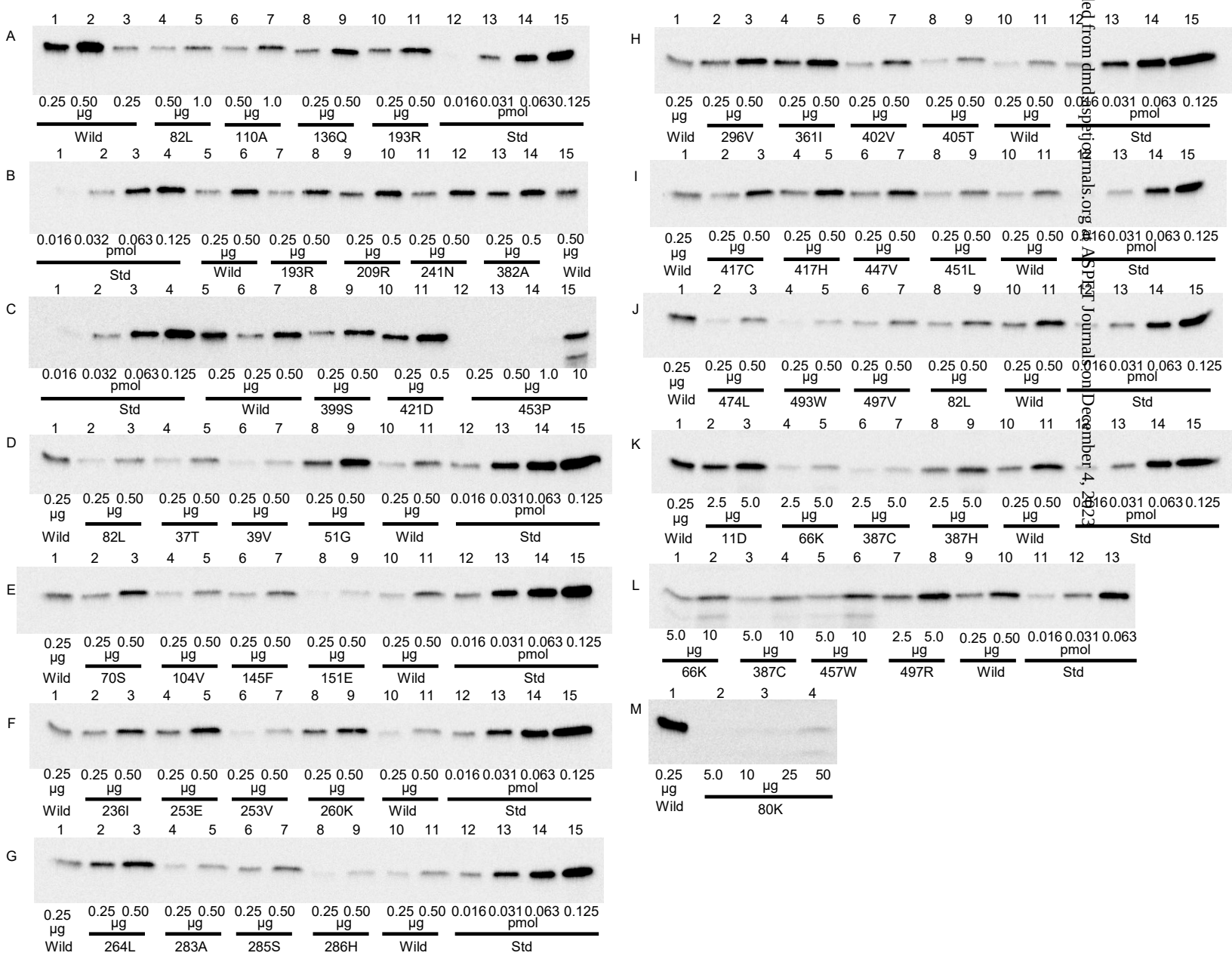

DMD Fast Forward. Published on April 11, 2023 as DOI: 10.1124/dmd.123.001310

Fig. 2

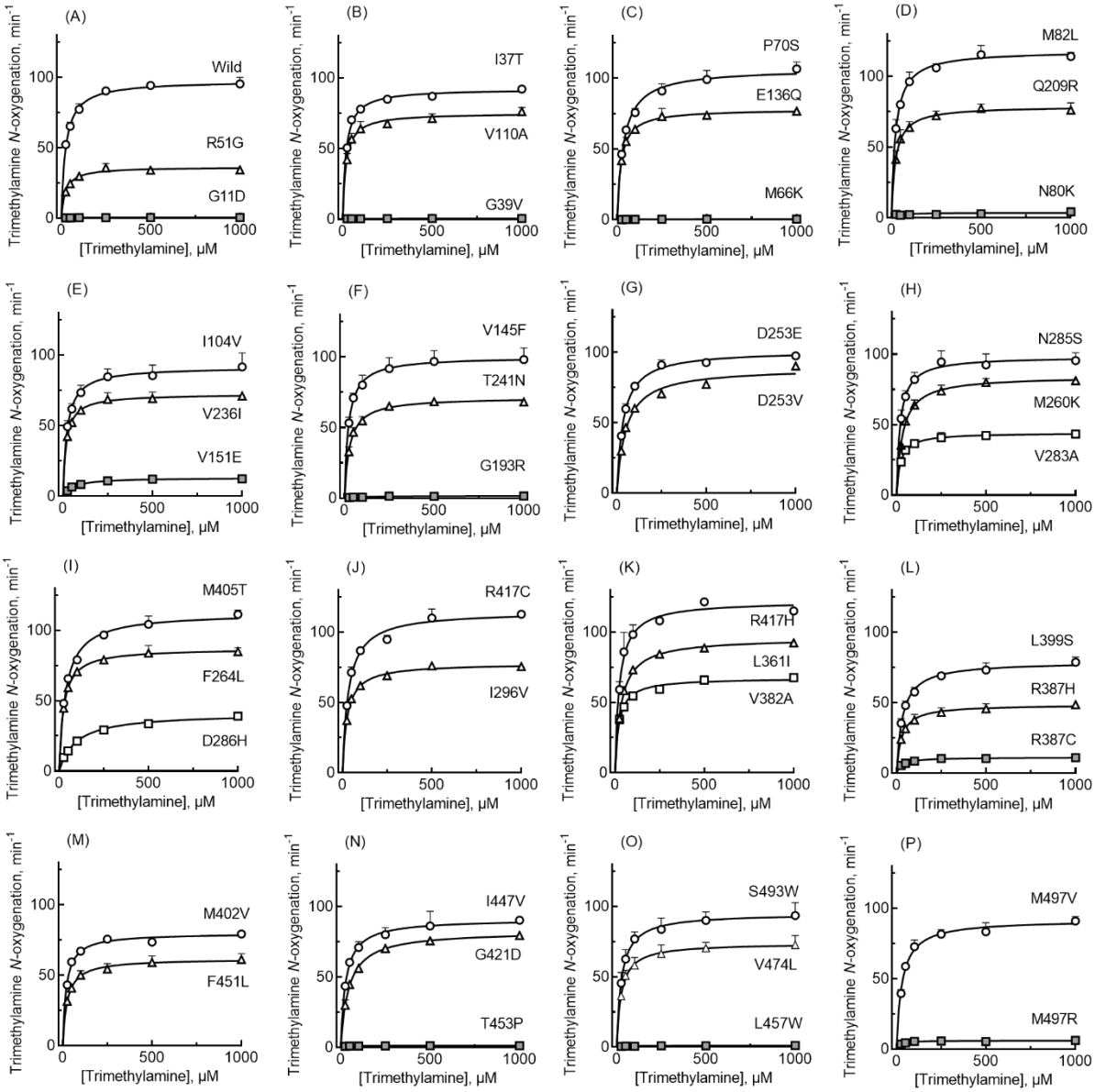

Fig. 3